Electronic Supplementary Material (ESI) for RSC Advances.
This journal is © The Royal Society of Chemistry 2015

Supporting Information

General Transfer Hydrogenation by Activating Ammonia-Borane over Cobalt Nanoparticles

Tian-Jian Zhao†, Ya-Nan Zhang†, Kai-Xue Wang, Juan Su, Xiao Wei, Xin-Hao Li*

School of Chemistry and Chemical Engineering, Shanghai Jiao Tong University, Shanghai 200240, People's Republic of China.

†These authors contribute equally to this work.

*e-mail: xinhaoli@sjtu.edu.cn

Chemicals: Cyanamide (Aldrich,50 wt% in H_2O, contains 0.1 % formic acid as stabilizer), Ludox HS40 solution (Alfa Aesar, Silicon(IV) oxide, 40 % in H_2O,colloidaldispersion), hydrofluoric acid (HF, Sinopharm Chemical Reagent Co., Ltd., ≥40.0%), ethanol (CH_3CH_2OH, Sinopharm Chemical Reagent Co., Ltd., ≥99.7%) Dicyandiamide (DCDA, Acros Organics, 99.5%), monohydrate glucose (AppliChem, pure Ph. Eur.).Ammonia-borane (AB, NH_3BH_3, Aldrich, 90%), cobalt (II) chloride hexahydrate ($CoCl_2{\cdot}6H_2O$, Sinopharm Chemical Reagent Co., Ltd., ≥99.0%). Acetylene black (C, carbon black, commercially available). Dichloromethane (CH_2Cl_2, Sinopharm Chemical Reagent Co., Ltd., ≥99.5%).

1. Procedure for catalyst preparation

Synthesis of 30 wt. % Co/CN: Mesoporous carbon nitride was obtained according to Ref. 30. Briefly, 5 g of cyanamide was dissolved in 7.5 g of Ludox HS40 solution (dispersion of 12-nm SiO_2 particles with 40 wt% in water) and heated at 65 °C overnight to remove water. The as-formed white powder was heated at a temperature of 600 °C for 4 h (ramp: 2.3 °C min^{-1}) under the protection of N_2. The resulting brown-yellow powder was treated with a 4 M HF acid for 24 h to remove the silica template. The powders were then centrifuged and washed three times with distilled water and twice with ethanol. Finally the powders were dried at 60 °C in vacuum overnight.

Then 14 mg of the as-prepared mpg-CN was dispersed into 9 mL distilled water with 24 mg of $CoCl_2{\cdot}6H_2O$ for about two days. And then 1 mL freshly prepared NH_3BH_3 aqueous solution (containing 2.68 mmol AB) was added while stirring at room temperature. The catalyst was separated by an external magnet and finally dried at 60 °C overnight. The mass percentages of Co were calculated on the basis of the weights of Co content in the precursor and mpg-CN.

Synthesis of 30 wt. % Co/N-LC: Nitrogen-doped layered carbon was obtained according to Ref. 39 In summary, a mixture of dicyandiamide (5 g) and glucose (1 g) was heated at a temperature of 900 °C for 1 hour (ramp: 2.3 °C min^{-1} under protecting N_2 flow. Then 14 mg of the as-formed N-LC was dispersed into 9 mL distilled water with 24 mg of $CoCl_2 \cdot 6H_2O$ for about two days. And then 1 mL freshly prepared NH_3BH_3 aqueous solution (containing 2.68 mmol AB) was added while stirring at room temperature. The catalyst was separated by an external magnet and finally dried at 60 °C overnight.

Synthesis of 30 wt. % Co/C: 14 mg of C was dispersed into 9 mL distilled water with 24 mg of $CoCl_2 \cdot 6H_2O$ for about two days. And then 1 mL freshly prepared NH_3BH_3 aqueous solution (containing 2.68 mmol AB) was added while stirring at room temperature. The catalyst was separated by an external magnet and finally dried at 60 °C overnight.

2. Catalyst characterization

The **TEM** and **HRTEM** measurements were taken with a JEM-2100F microscope operated at an acceleration voltage of 200 kV. **Nitrogen sorption** experiments were performed with a Quadrasorb at 77 K, and data analysis was performed with Quantachrome software. Samples were degassed at 150 °C for 20 h before measurements. The **PXRD** measurements were performed on a Rigaku D/Max 2550 X-ray diffractometer operating at the Cu Kα1 radiation. The photoluminescence (**PL**) emission spectra were recorded on a QM-4-CW (Photo technology international, Int.USA/CAN). The **FTIR** spectra were recorded using a Bruker IFS 66v/S FTIR spectrometer equipped with a deuterated triglycine sulfate (DTGS) detector. The **UV-vis** spectrophotometer (UV-3600) was employed to obtain the diffuse reflectance spectra of the samples.The **GC** analysis was performed on Shimadzu GC-2014 gas chromatograph.

3. Catalytic Study of the catalysts

Catalytic reduction of nitrobenzene

1 mL freshly prepared NH_3BH_3 aqueous solution (containing 2.68 mmol AB) was added into the suspension consisting of g-C_3N_4, and $CoCl_2$ (see the Synthesis of Co/CN) while stirring at room temperature under ambient atmosphere. At the same time, the as-formed H_2 was monitored by a gas burette system. Quantitative (0.5 mmol) substrate was added into the suspension consisting of 2 mmol AB and 20 mg catalyst when the H_2 production reached 30 ml. After the hydrogen generation reaction was complete, the catalyst was separated by an external magnet. The sample obtained by extraction in CH_2Cl_2 was directly subjected to GC analysis. Conversion and yields were determined by GC-FID (HP6890 with FID detector, column HP530 m x 250 mm x 0.25 μm).

Stability of 30 wt. % Co/CN catalyst: After the hydrogen generation reaction was completed, the sample was separated by extraction in CH_2Cl_2 while the catalyst was separated by an external magnet. Then the equivalent of AB (92 mg) and nitrobenzene (0.5 mmol) were added to the reaction system. After the hydrogen generation reaction was completed, the catalyst was separated by an external magnet. The sample obtained by extraction in CH_2Cl_2 was directly subjected to GC analysis. Conversion and yields were determined by GC-FID (HP6890 with FID detector, column HP530 m x 250 mm x 0.25 μm).

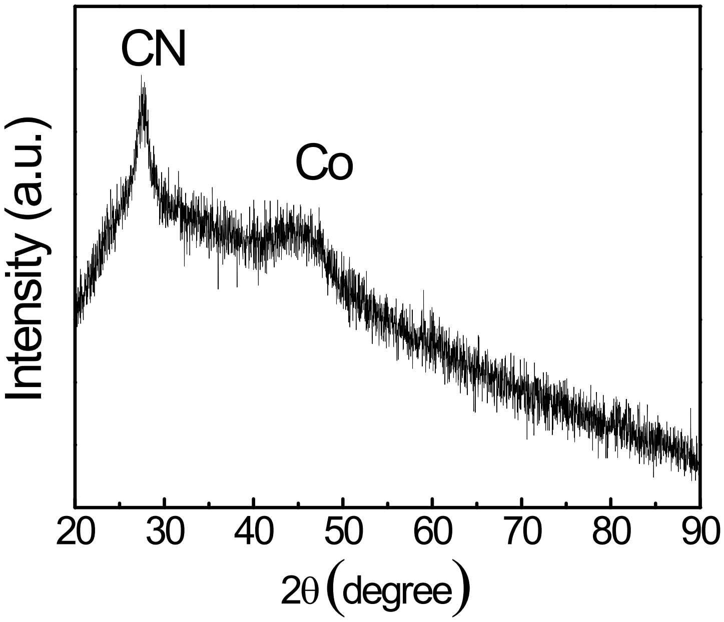

Figure S1. XRD profiles for Co/CN catalyst. The weight percentage of the Co component is 30% for the sample. The intensity of peaks of the Co metals is relatively weak, due to the small size of crystal domains of metallic cobalt, as demonstrated by further HRTEM observation.

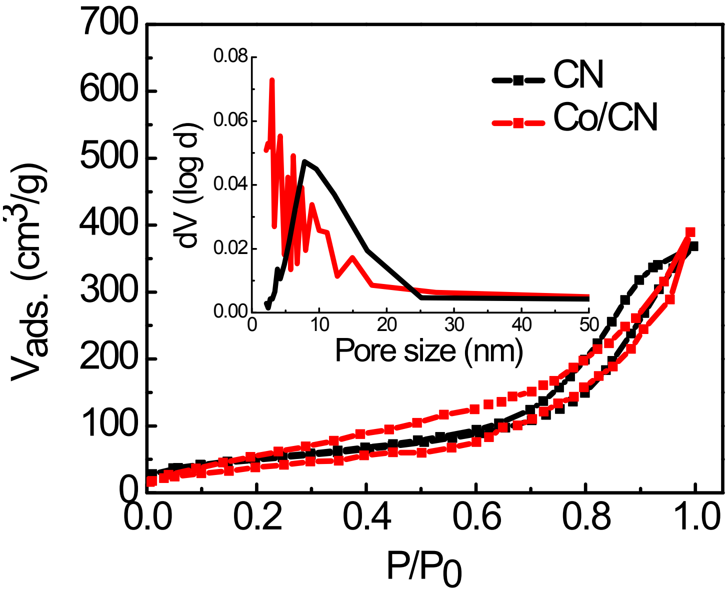

Figure S2. Nitrogen sorption isotherms of bare CN and 30 wt. % Co/CN catalyst. Inset: corresponding pore-size distributions. There is a decrease in both surface area and pore size after the introduction of metal cobalt, suggesting the successful loading of cobalt nanoparticles.

Table S1. BET surface area and Pore size of CN and Co/CN.

Sample	Surface area (m^2/g)	Pore size (nm)
CN	177.761	7.811
Co/CN	151.434	2.988

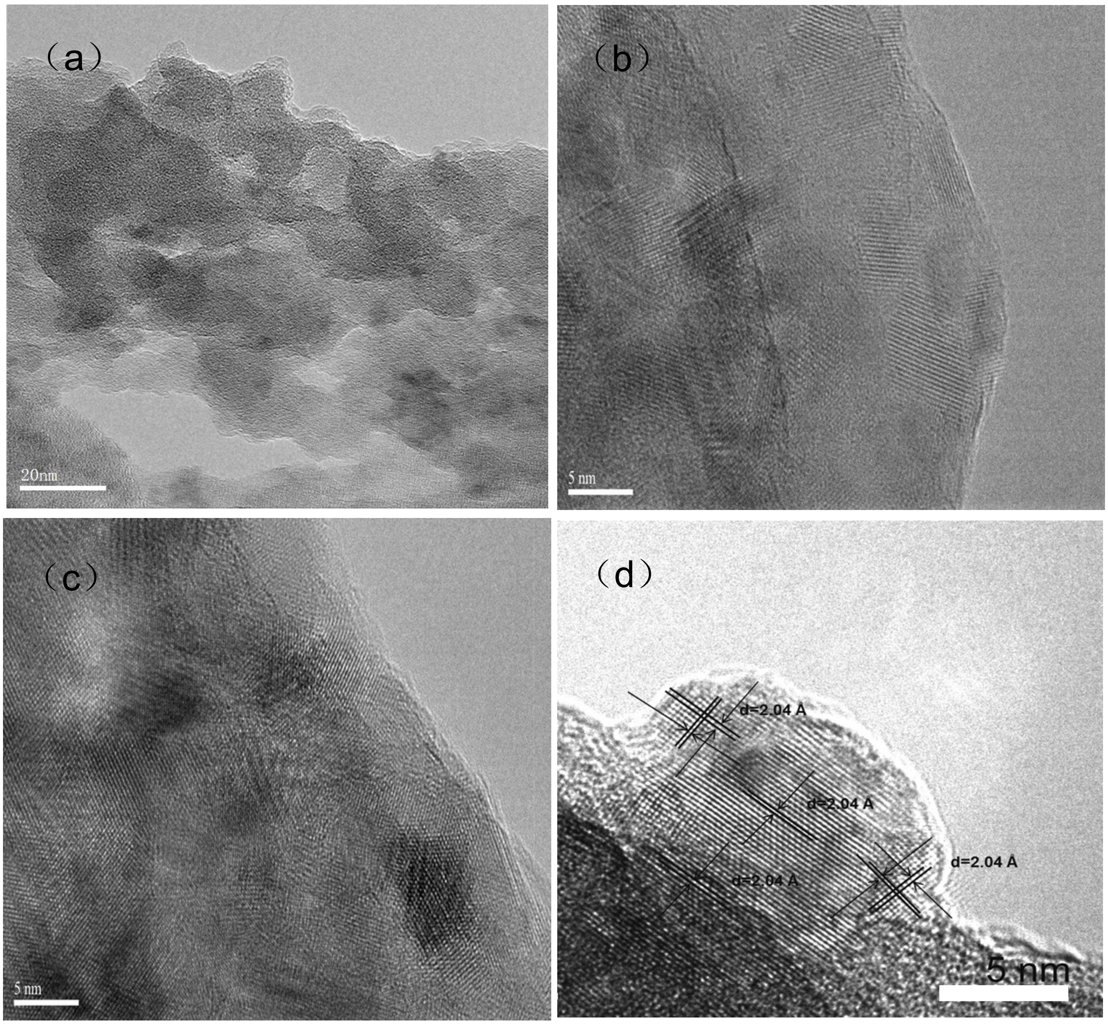

Figure S3. The presence of Co components could not be distinguished by low-magnification transmission electron microscopy (TEM) observation (a) due to the similar contrast between Co species and CN components. Nevertheless, the well preservation of the porous structure was confirmed by TEM image after loading Co nanoparticles. HRTEM images of Co NPs formed on the surface of CN support. Typical HRTEM image (b c and d) confirms the formation of metallic Co nanoparticles with a fringe spacing of about 0.204 nm, which can be attributed to the (111) facet of Co metal. The size of primary Co nanocrystals was ranged from 2 to 10 nm.

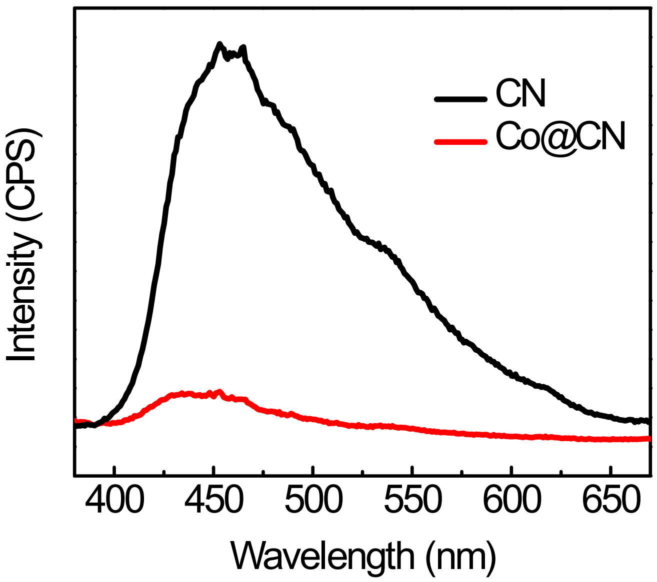

Figure S4. Photoluminescence (PL) spectra of bare mesoporous carbon nitride (CN) and 30 wt. % Co/CN catalyst. The decreased photoluminescence intensity (red line) of carbon nitride after the introduction of Co NPs is indicative of electron transfer from carbon nitride to Co NPs.

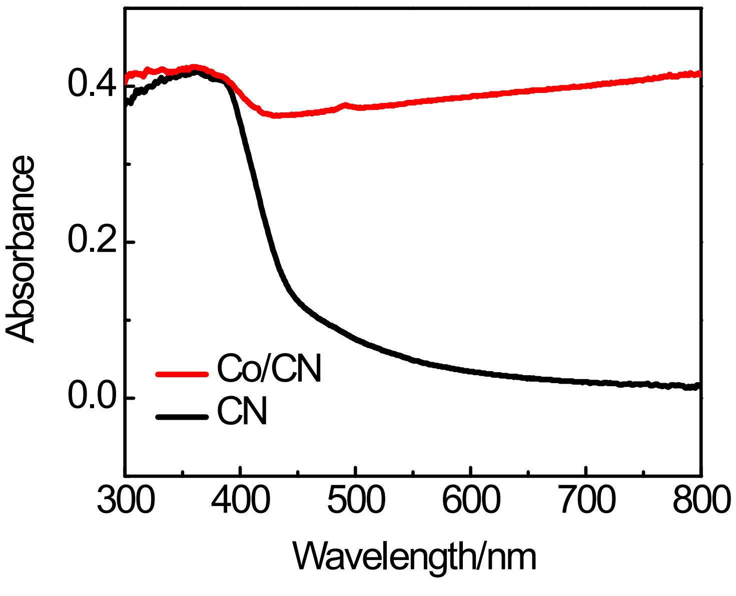

Figure S5. UV-Vis adsorption spectra of 30 wt. % Co/CN and bare carbon nitride (CN). The complete absorption (red line) of 30 wt. % Co/CN catalyst is the absorption of Co NPs.

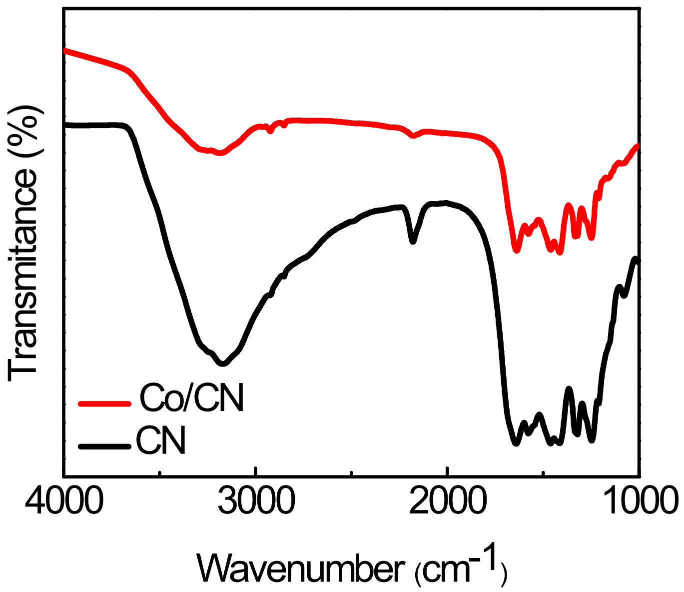

Figure S6. FTIR profiles for bare mesoporous carbon nitride (CN), 30 wt. % Co/CN catalyst. The infrared absorption around 3200 cm^{-1} is indicative of secondary and primary amines. The peaks of C−N heterocycle stretches of the extended network connection in the 1100−1600 cm^{-1} region are also very strong and sharp, again indicating development of the polymeric melon network in g-C_3N_4. There was no obvious change in CN after the introduction of metal cobalt, suggesting the excellent stability of CN.

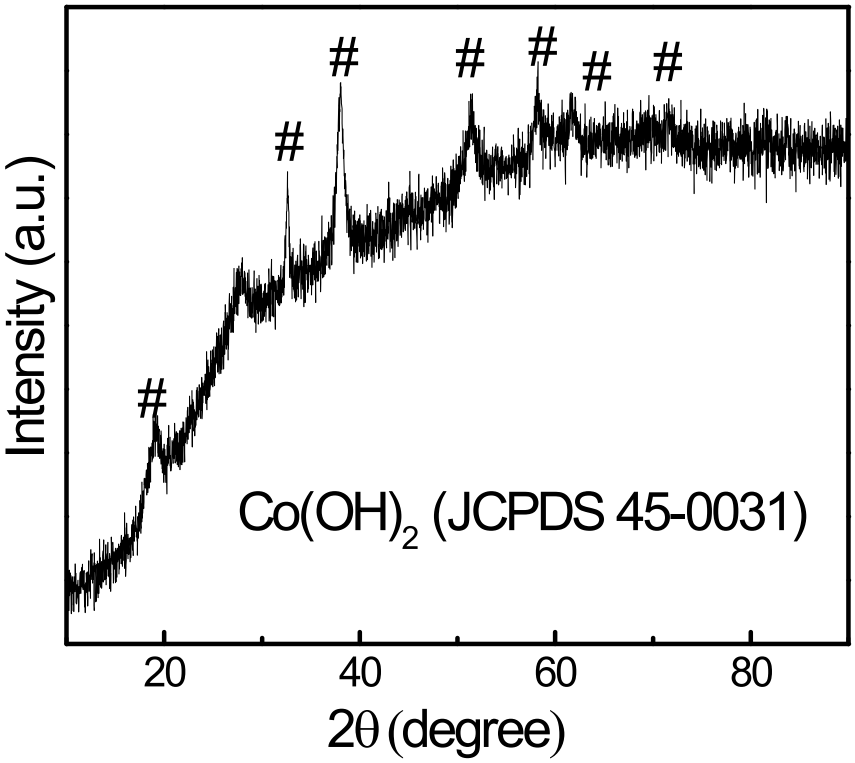

Figure S7. XRD pattern of $Co(OH)_2$/CN sample, excluding the presence of Co^0 species.

Table S2. Effect of Co loadings on the activity of Co/CN catalyst in the reduction of nitrobenzene. [a]

Entry[a]	Catalyst	Conv.[%]	Sel.[%]
1	5wt.% Co/CN	2	56 [b]
2	20wt.% Co/CN	43	>99
3	30wt.% Co/CN	>99	>99
4	40wt.% Co/CN	36	82[b]

[a]Reaction condition: 0.5 mmol nitrobenzene, 10 mL of water, 20 mg of catalyst, 2 mmol NH_3BH_3, room temperature, 5 min. [b]The byproduct is nitrosobenzene.

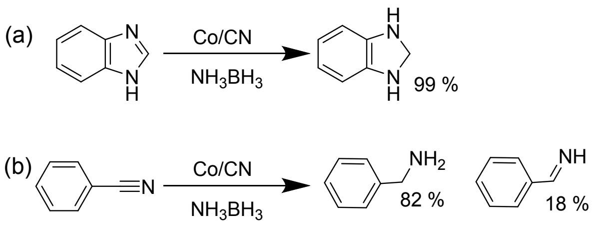

Scheme S1. Transfer hydrogenation of benzimidazole (a) and cyanobenzene (b) using Co/CN and AB. (a) Reaction conditions: 0.5 mmol substrate, 10 mL of water, 20 mg of 30% Co/CN, 2 mmol NH_3BH_3, room temperature, 15 min. (b) Reaction conditions: 0.25 mmol substrate, 10 mL of water, 20 mg of 30% Co/CN, 2 mmol NH_3BH_3, room temperature, 12 h.

Table S3. Scalability of the catalytic system over Co/CN.

Substrate	Product (yields / %)	Time
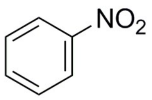	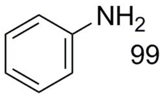 99 %	10 min
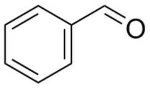	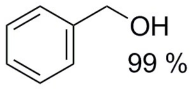 99 %	10 min
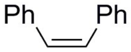	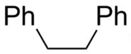 99 %	10 min
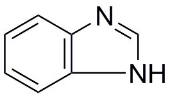	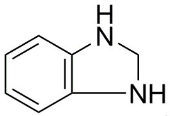 99 %	10 min
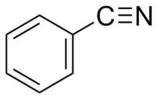	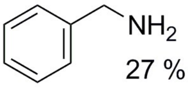 27 % 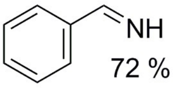 72 %	12 h

Reaction condition: 5 mmol substrate, 100 mL of water, 200 mg of catalyst, 20 mmol NH_3BH_3, room temperature.

For most substrates, both conversions and selectivity of scaled-up reactions comparable to those of standard reactions. For hydrogenation of cyanobenzene, an obvious decrease in the selectivity to benzylamine was observed in 10-times scale-up synthesis, presumably due to the fast decomposition of AB into hydrogen gas. In principle, the selectivity to benzylamine could be improved via successively adding AB into the catalytic system, which is however not within the scope of this research.

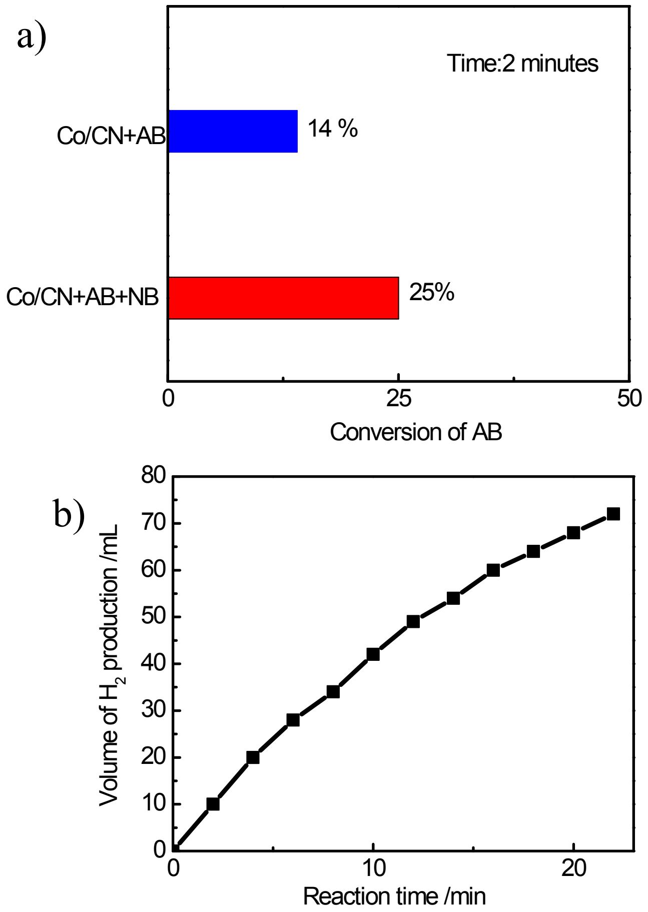

Figure S8. AB conversion with or without nitrobenzene (NB) over Co/CN (A). Under optimized conditions, complete conversion of nitrobenzene can be achieved within 2 minutes. When nitrobenzene was not involved, 10 mL of H_2 forms (B) in our catalytic system via the decomposition of AB. The conversion of AB is 14%. Such a conversion is little lower than the reaction with the presence of nitrobenzene, which converts more than 25% of the AB as calculated from the amount of aniline detected.

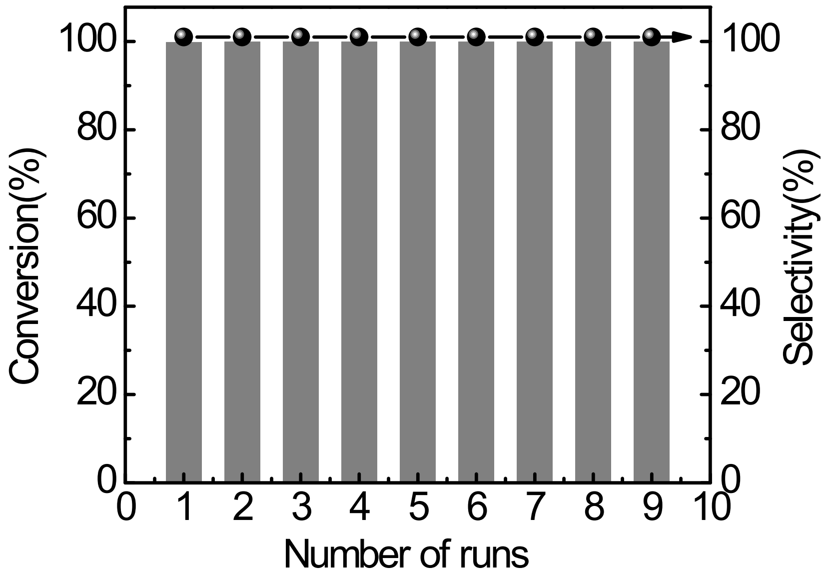

Figure S9. Conversion of nitrobenzene over used 30 wt. % Co/CN. Excellent conversion and selectivity can be achieved through nine cycles. The carbon balance of all these reactions were demonstrated to be 95-101 %, further suggesting the complete conversion of nitrobenzene to aniline.

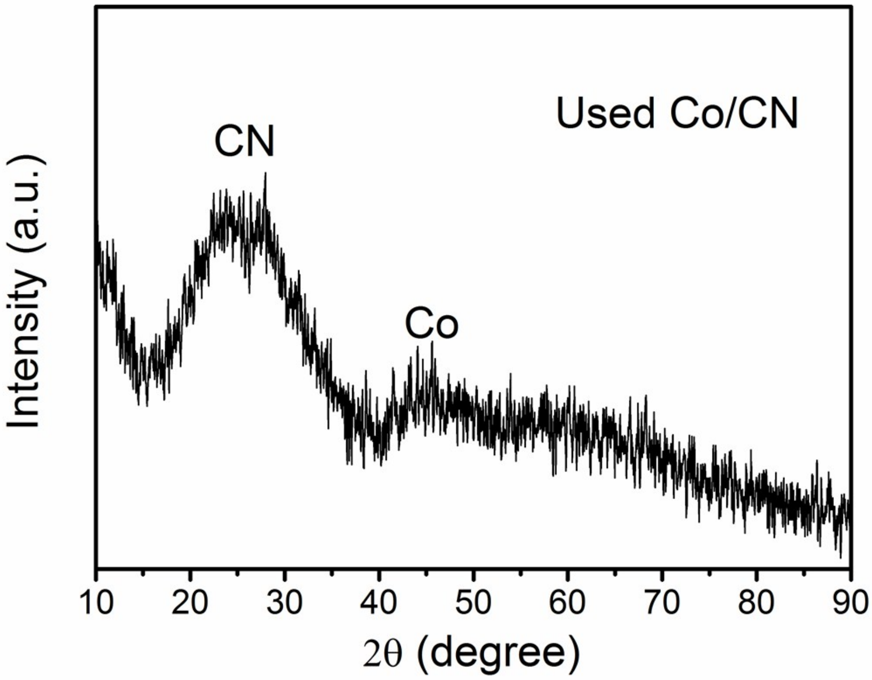

Figure S10. XRD pattern for used Co/CN catalyst (after 1st run). After multiple uses, the typical peak of metal Co components became weaker as compared with that of fresh sample. Considering the reductive environment of our catalytic system, we could exclude the effect of oxygen on such a decrease in crystallinity of metallic Co components. Activating AB over Co/CN should principally proceed via a reversible conversion between Co^0 and Co^{2+} (in the form of cobalt hydride) species, resulting in obvious decrease in the crystallinity of metallic Co components accordingly. However, the catalytic activity of Co/CN was not disturbed obviously in following runs as shown in Figure S8. This is to say that neither metallic nor $Co(OH)_2$ components were catalytic active centers in Co/CN sample. All these results rather suggested the key importance of Co^0/Co^{2+} pairs in Co/CN for activating AB and hydrogenation of unsaturated organic compounds here.

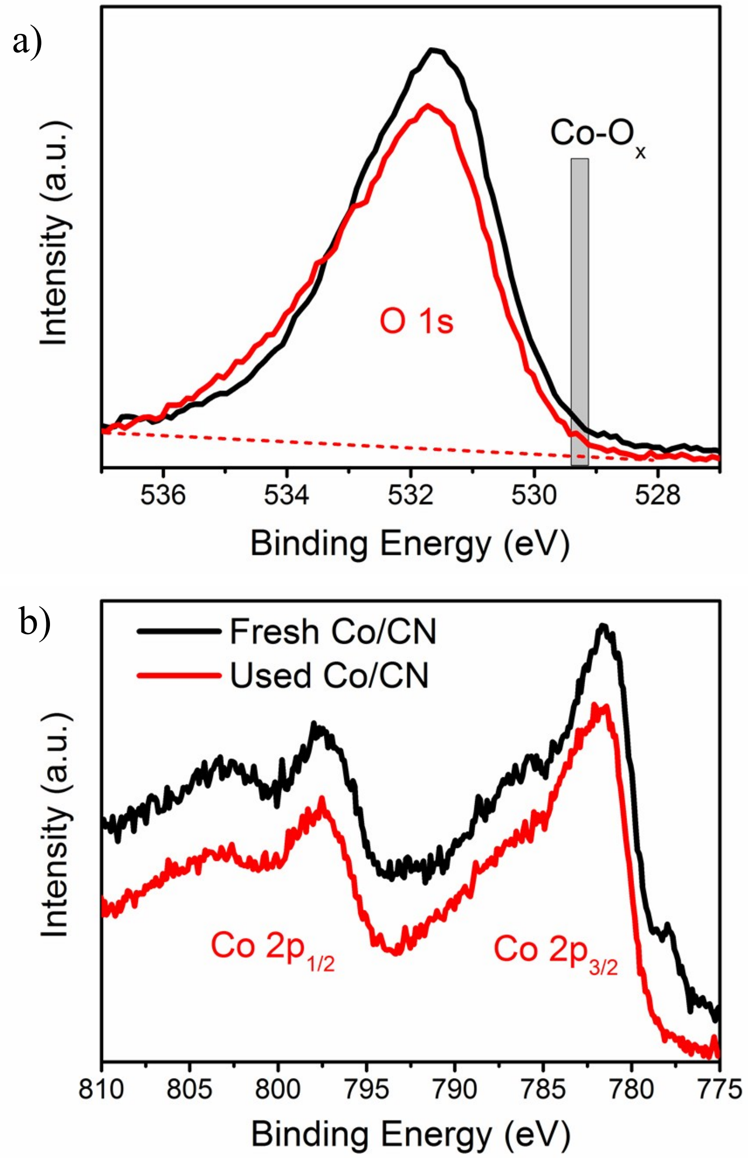

Figure S11. XPS O 1s (a) and Co 2p (b) spectra of fresh and used Co/CN catalysts. After catalytic reaction, the chemical structure of Co components was not obviously altered. This phenomenon explains the excellent reusability of Co/CN catalysts, even though the crystallinity of metallic Co components decreases slightly. This result again demonstrated the key role of Co^0/Co^{2+} containing Co/CN dyad for activating AB and triggering further hydrogenation reactions in a general but highly selective style.

Table S4. Transfer hydrogenation of unsaturated halogenated compounds over Pd/CN catalyst.

Substrate	**Product**			
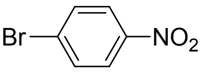	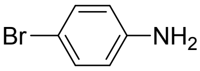	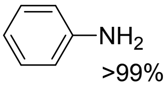 >99%		
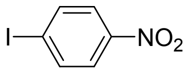	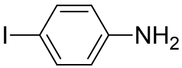 0.1%	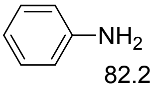 82.2%	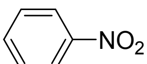 13.1%	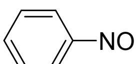 4.6%
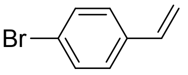	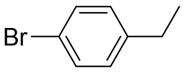	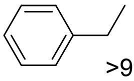 >99%		
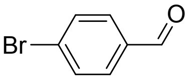	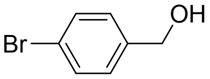	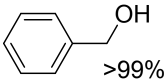 >99%		
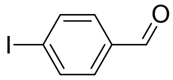	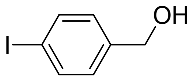	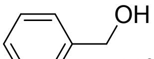 >99%		
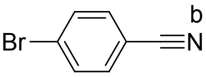	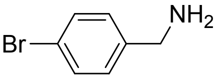	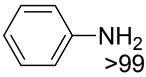 >99%		
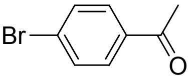	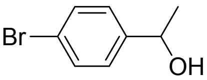	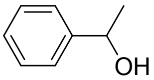 >99%		
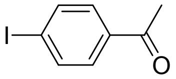	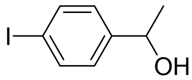	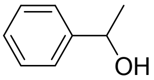 >99%		

[a]Reaction condition: 0.5 mmol substrate, 10 mL of water, 20 mg of catalyst, 2 mmol NH_3BH_3, room temperature. [b]0.25 mmol substrate.